Chapter 4
Ferrite Nanoparticles for Water Decontamination Applications

Aayush Gupta and Raveena Choudhary

1 Need of Wastewater Treatment

> "If we move forward and don't clean up the messes of the past, they'll just get swept under the rug."—Erin Brokovich.

Water is a source of survival for all forms of life on earth. One cannot die without love and surely can without water. Globally, the supply of safe, secure, and inexpensive water has been one of the biggest difficulties faced in recent years. Fresh water availability per capita has been decreased as a result of the alarming rate of industrialization and population growth [1, 2]. Water covers over 71% of the surface of the globe. Of the total available water, around 97% is found in oceans and 3% is fresh water. Only 0.3% of the freshwater on earth's surface is located in fresh lakes, rivers, and streams, while 68.7% of the remaining fresh water is frozen in icecaps and glaciers. The remaining freshwater is found beneath the ground [2]. The water distribution over the earth's surface is depicted in a pie chart in Fig. 1.

Along with the very low availability of fresh water on the earth, industrialization and urbanization are also causing the deterioration of water quality. As a result, water crises are becoming unimaginably severe over the globe. Even though the planet's freshwater supply has mostly remained steady over time through constant recycling via the atmosphere and back. The rise in population implies that the rivalry for a plentiful supply of clean water for drinking, cooking, bathing, and supporting life grows more intense every year. According to a recent report by UNICEF, nearly 2/3rd of the world's population, i.e., 4.0 billion people endure extreme water scarcity for at

A. Gupta (✉)
Department of Mechanical Engineering, GLA University, Mathura 281406, India
e-mail: present.ayush@gmail.com

R. Choudhary
School of Physics and Materials Science, Thapar Institute of Engineering and Technology, Patiala 147004, India

P. Sharma et al. (eds.), *Engineered Ferrites and Their Applications*, Materials Horizons: From Nature to Nanomaterials, https://doi.org/10.1007/978-981-99-2583-4_4

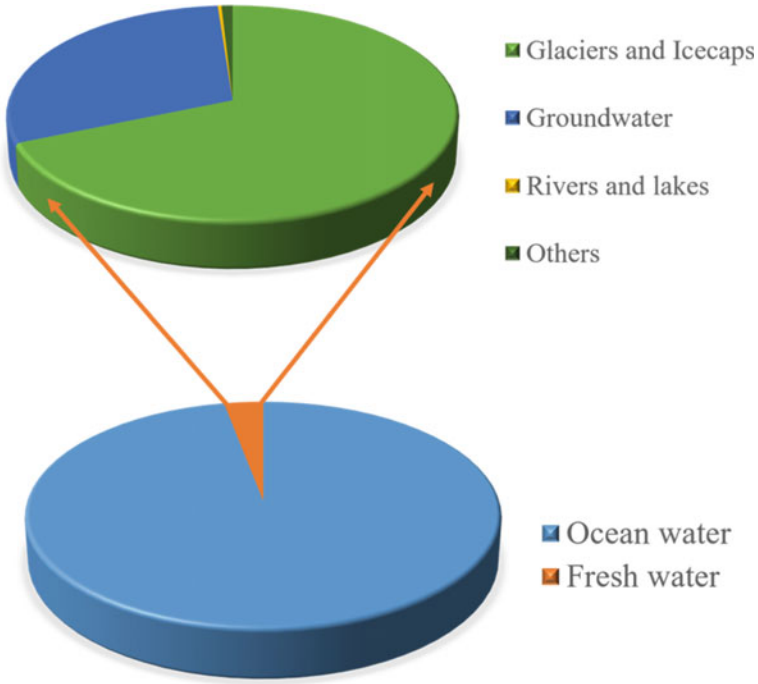

Fig. 1 Water distribution over the earth's surface

least one month each year. Due to the acute water shortage, 700 million people may be displaced worldwide by 2030 [3]. These key factors of water scarcity in the future are enough to be alarmed and step up for water conservation. Due to the dumping of polluted water effluents from industries to rivers and other freshwater streams, water-borne diseases are rising. According to recent data from a WHO assessment, at least 2 billion people drink polluted (feces) water. Microbial contamination brought on by feces contamination poses the biggest threat to the potable water. Drinking water contaminated by microorganisms increases the risk of contracting diseases such as diarrhea, cholera, typhoid, polio and contributes to the 4,85,000 annual deaths from diarrhea. The most dangerous chemicals in drinking water include arsenic, fluoride, and nitrate, but novel pollutants like pesticides, drugs, per- and polyfluoroalkyl substances (PFASs), and microplastics are now a source of public concern [4]. These pollutants generally emerge from wastewater from industries and households. Recycling wastewater effluents is therefore a top issue in every community worldwide in terms of environmental conservation and sustainable development.

2 Background of Photocatalytic Wastewater Treatment

The major water pollutants are of three types, viz. organic, inorganic, and microbial contaminants. The organic pollutants include pesticides, phthalates, phenols, dyes, and other VOCs from industries. These pollutants are usually carcinogenic and mutagenic in nature even present in very small fractions and can lower dissolved oxygen causing harm to humans and aquatic life. Metals, salts, and other substances free of carbon are examples of inorganic pollutants. From an ecotoxicological point of view, metal ions like Hg^{2+}, Pb^{2+}, Cr^{3+}, Cr^{4+}, Ni^{2+}, Co^{2+}, Cu^{2+}, Cd^{2+}, Ag^{+}, As^{5+}, and As^{3+} are toxic. In addition, the contamination caused by radioactive elements is a serious problem given their potentially dangerous long-term effects. Microbes/pathogens including bacteria, viruses, and parasites may only be present in very small concentrations in drinking water, but they are a major risk factor for the safety of water since they spread many infectious diseases. The pathogens such as bacteria, viruses, protozoa, and helminths are responsible for disease such as diarrhea, cholera, gastrointestinal illness [5–13].

Primary, secondary, and tertiary treatments are some of the processes in the treatment of wastewater as shown in Fig. 2. In the preliminary treatment procedure, heavy objects like sand, stones, etc. are separated from water using a range of processes, such as screening followed by grit removal, then pre-aeration, flow metering, and finally sampling. After initial treatment, primary treatment using sedimentation and floatation process removes the settleable organic solids. Biological techniques are employed in secondary treatment to further decompose organic materials, remove dissolved and colloidal particles (aquatic microorganisms). The most important and final stage entails a thorough tertiary treatment to clean the secondary-treated water and make it fit for consumption [14, 15]. There are tertiary treatments available to extract or degrade waste from wastewater using physical, chemical, and biological techniques (Fig. 2). These methods include electrochemical techniques, ozonation, adsorption, reverse osmosis, coagulation and flocculation, precipitation, and fungal decolonization [16–22]. For tertiary treatment, typical purification systems are either inefficient or excessively expensive. When using chemical techniques, ozonation is the least effective because of its short life and high expense, while the limitation of chlorination is that it may produce trihalomethane, a harmful disinfection by-product. Reverse osmosis is an expensive and ineffective physical approach for treating wastewater, as are flocculation and filtering [23]. When using biological methods, system handling becomes extremely important. Therefore, there is still a need for an effective, affordable, and manageable wastewater treatment method.

Among various wastewater treatment techniques, advanced oxidation process (AOP) compared to other techniques is rapid, effective, and inexpensive. It can overcome obstacles including hazardous by-products, high costs, and partial removal of pollutants. AOPs are employed for the complete mineralization of complex biorefractory pollutants from aqueous solution [1]. Different AOPs include Fenton-like reactions, ozonation, and photocatalysis which require costly catalysts, equipment and may lead to incomplete degradation to form toxic secondary products which adds

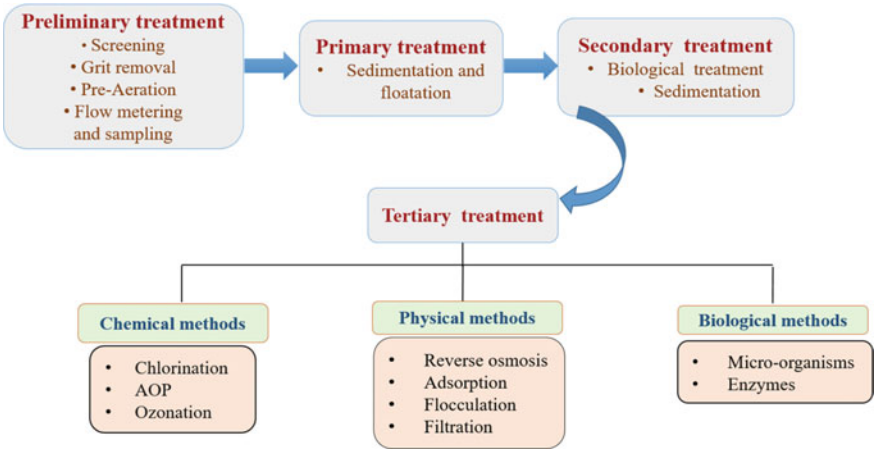

Fig. 2 Wastewater treatment stages

to environmental stress. One form of promising AOP technology is sunlight-driven photocatalysis. Solar irradiation has the ability to activate photocatalysts, resulting in the production of highly reactive photo-induced charge carriers that react with contaminants. In AOP photocatalytic process, the photocatalyst is generally mixed with the aqueous sample in which pollutants are present. The mechanism of photocatalysis is shown in Fig. 3. The basic principle on which AOP photocatalysis works involves the generation of exciton pair upon irradiation exposure of photocatalyst with electromagnetic radiation of energy, equal or greater than the optical band gap of the catalyst. The transition of electron (e^-) from the valence band to the conduction band occurs, and holes (h^+) are left in the valence band. Therefore, a photocatalyst with a smaller band gap is more likely to absorb more photons from visible light. The generated e^- and h^+ further react with water and dissolved oxygen in the water to form superoxide anion radicals and hydroxyl radicals. These radicals further react on the adsorbed pollutant on the surface of the catalyst to decompose it to form minerals and CO_2 [24]. The following equations represent the mechanism of photocatalysis:

$$\text{catalyst} + h\nu \rightarrow \text{catalst} + \text{h}^+ + \text{e}^-, \tag{1}$$

$$\text{catalyst}\left(\text{e}^-\right) + \text{O}_2 \rightarrow \text{O}_2^-, \tag{2}$$

$$\text{catalyst}\left(\text{h}^+\right) + \text{H}_2\text{O} \rightarrow \text{OH}^{\cdot}, \tag{3}$$

$$\text{O}_2^- + \text{OH}^{\cdot} + \text{pollutant} \rightarrow \text{CO}_2 + \text{H}_2\text{O}. \tag{4}$$

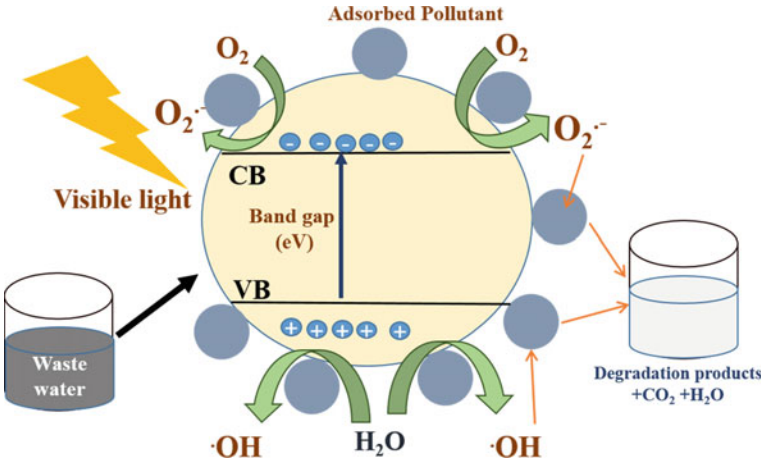

Fig. 3 Mechanism of photocatalytic wastewater treatment

3 Magnetic Materials as Photocatalyst

There are variety of materials which have been used so far as photocatalyst for wastewater treatment including metal oxide (ZnO, TiO_2, $BiTiO_3$, $SrTiO_3$, Fe_2O_3, BiOBr, $CaFe_2O_4$, $ZnFe_2O_4$, etc.), metal organic frameworks, carbon nanostructures (carbon nanosphere, carbon nanotube, carbon nitride, etc.), metal sulfide (ZnS, CdS, $CuInS_2$, etc.), piezoelectric materials, and noble metals (Pt, Ag, and Au). Due to its great chemical inertness, non-toxicity, abundance (0.44% of the earth's crust), and cost, titanium dioxide (TiO_2) is currently the most used photocatalyst. Possessing 3.2 eV as optical band gap, TiO_2 can absorb UV light ($\lambda < 387$ nm), which only makes up 5–8% of the whole solar spectrum. As a result, efforts have made on developing novel composite of TiO_2 with various components, such as carbon nanotubes, activated carbons, metal ions (Co, Ag, Au, etc.), and non-metals (nitrogen, carbon, sulfur, etc.). A good photocatalyst needs to have a low bandgap energy, with CB and VB at the proper positions to increase visible light activity. Other than that, a common problem with all the photocatalysts is their recovery from solution after use and thereafter their reuse, which restricts the scope of applications for photocatalysis [25–27].

Recently, magnetic materials have proven to be more useful for application of photocatalysis. The advantages of magnetic materials as photocatalysts over non-magnetic photocatalysts are their high efficiency, sustainability, and ease of preparation. When the particle size decreases (to nano-level), solid/liquid separation becomes increasingly challenging. On the other hand, magnetic filtering can be used for separation of catalyst from solution when using magnetic sorbents based on metal oxides. Additionally, using magnetic fields to remove particles from solutions is more efficient and effective (and frequently much faster) than centrifugation or filtering. The benefits of employing magnetic nanoparticles as an adsorbent in water treatment procedures include their high reusability, biocompatibility, selective solid/liquid

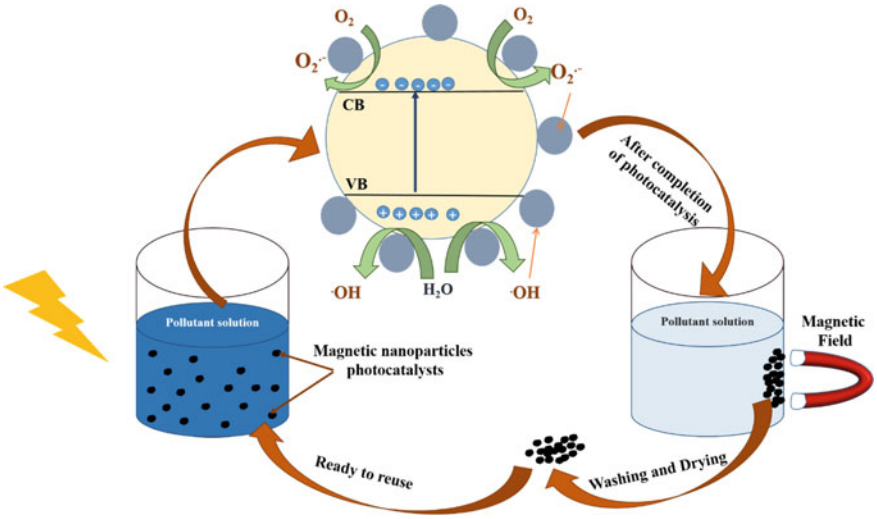

Fig. 4 Illustration of photocatalysis and removal of magnetic nanoparticles

separation using magnetic filtration, which is speedier than centrifugation and filtration procedures. However, the most important advantage of using magnetic materials is that catalysts are simply removed using a magnetic field from outside to separate the reaction liquid [28, 29]. The entire processes can be done with low cost in less time and improved reusability of the catalyst (Fig. 4).

Numerous types of magnetic materials have been fabricated, developed, and employed successfully in a variety of applications, including biomedicine, MRI, catalysis, spintronics, robotics, engineering, environmental remediation, etc. [2]. For a magnetic material being able to show best photocatalytic behavior under visible light, the following conditions must be satisfied:

- Their band gap should lie in the region of semiconductor (2–3 eV).
- Should be applicable at ambient temperature and pressures.
- Good selective adsorption.
- Lower rate of recombination of electrons and holes.
- Complete mineralization with no harmful by-products.

There are several methods to synthesize magnetic materials, including co-precipitation, solvothermal, hydrothermal, microemulsion, sonochemical, etc., which affect their magnetic properties, particle size, distribution, shape, and other characteristics. There are variety of metals which show magnetic properties, but the strongest magnetic materials consists of iron, cobalt, and nickel or their alloys [2]. All these magnetic photocatalysts are typically the composites made of magnetic material and non-magnetic photocatalytic material. In general, iron is used as one of the major components for the synthesis of magnetic photocatalysts. The most common and potentially useful magnetic minerals for water treatment are α-Fe_2O_3 (hematite),

β-Fe_2O_3 (maghemite), Fe_3O_4 (magnetite), and FeO (wustite) out of the eight known phases of iron oxides [30]. Initially, single-phase magnetic material such as Fe_2O_3 is used in environmental applications [31]. Rarely, reports are there on magnetic photocatalysts with a single phase that had high catalytic performance [32]. Most single-component, single-phase photocatalysts have a weak capacity for visible adsorption, which results in a low catalytic efficiency. Development of binary and ternary photoactive ferrites has been used to address this difficulty. The general formula for a material containing Fe^{3+} is MFe_2O_4, where M is a transition metal (Cu, Zn, Co, Mn, Ba, or Ni). Size- and shape-dependent magnetic response (saturation magnetization) of ferrites enables their utility as photocatalyst under external magnetic field. In terms of a photocatalytic application, the narrow band gap caused by the additional metal (M) enables ferrite as a very potent catalyst under visible radiation. Strong photocatalytic activity is demonstrated by ferrites, particularly when paired with other binary or photoactive materials such as $BiFeO_3$, $ZnFe_2O_4$, $CoFe_2O_4$, $NiFe_2O_4$ [33]. The examples of other binary ferrite photocatalysts along with synthesis method, pollutant, and efficiency of degradation are given in Table 1.

The interaction of a magnetic oxide with other oxide phase has also been extensively investigated as a way to produce highly photoactive materials. The catalytic activity can be significantly increased and charge recombination can be reduced when two different oxides are combined. Other than that, to overcome the difficulty of separation of photocatalyst along with the achievement of superior efficiency, combination of already available photocatalysts with the magnetic materials is came into existence. As TiO_2 is the most widely used catalyst, synthesis of magnetic photocatalyst in combination with TiO_2 has been studied broadly. For the very first time in 1994, Japanese patented the synthesis of Fe_3O_4/TiO_2 nanocomposites via titanium oxide deposition onto a magnetic core via hydrolysis of $TiOSO_4$, which led to its precipitation. Towata et al. in 1997 patented the dispersion of ferromagnetic particles in a TiO_2 suspension led to the creation of another magnetic photocatalyst [34]. Afterward, various researchers reported the deposition of photocatalyst onto magnetic core particles [35–38]. According to Beydoun et al. [35], charge carrier recombination of Fe_3O_4 could be caused by the contacts between the Fe oxide (core) and TiO_2 (shell) during illumination. Iron is less likely to be transported into the lower conduction band of the Fe_3O_4 core due to photogenerated electrons which are elevated to the conduction band of TiO_2. The iron oxide core's conduction band is preferred by the photogenerated holes in the valence band of TiO_2, which causes iron to oxidize and then leach iron ions into the solution. Therefore, it was concluded that interaction between magnetic Fe oxide and photoactive TiO_2 caused reduced photocatalytic activity when compared to solo TiO_2 against organic pollutant degradation. It was recommended to sandwich an inert layer between the magnetic core and TiO_2 shell to fend off photo-dissolution. The three-component photocatalyst is composed of three layers: (i) magnetic core, (ii) interlayer that prevents photo-dissolution and charge carrier recombination, and (iii) photocatalytic outer layer for the degradation of target molecule. Gad-Allah et al. [39] synthesized $TiO_2/SiO_2/Fe_3O_4$ composite as a magnetic photocatalyst in which silica was used as inert layer between TiO_2 and Fe_3O_4 to protect the magnetic and recombination of electron holes. In a similar

Table 1 Magnetic metal oxide-based photocatalysts with synthesis method, pollutant, and efficiency of degradation

Catalyst	Synthesis method	Saturation magnetization (emu/g)	Pollutant	Photocatalytic efficiency (%)	Ref.
Fe_3O_4@TiO_2	Hydrothermal	32.9	RhB	85	[43]
Fe_3O_4@MnO_2	Hydrothermal	–	Metal cations	88	[44]
$BiFeO_3$	Thermolysis	–	Doxorubicin	79	[45]
$ZnFe_2O_4$	Probe sonication	–	Acid red	98	[46]
$CoFe_2O_4$	Sol–gel	–	Reactive red	74	[47]
$NiFe_2O_4$	Co precipitation	31	Titan yellow	98.8	[48]
Fe_3O_4@ZnO	Hydrothermal	60.7	Phosphorous	92	[49]
Fe_3O_4@SnO_2	Hydrothermal	1.5	E. Coli inactivation		[50]
Fe_3O_4/g-C_3N_4	Hydrothermal	47.6	MB	98	[51]
Fe_3O_4@TiO_2	Sol–gel	–	Quinoline	95.6	[52]
Fe_3O_4@α-MnO_2	Two-step hydrothermal	39.9	BPA	92	[53]
Fe_3O_4@ZnO	Coprecipitation	24.2	AMX	90	[54]
rGO@Fe_3O_4@TiO_2	Sol–gel	–	MB	99	[55]
Fe_3O_4@MnO_2	Hydrothermal	32	Congo red	95	[56]
Cu@Fe@F_3O_4	Ball milling	38.56	MB	100	[57]
$CoFe_2O_4$	Wet chemical	–	4-nitrophenol	63	[58]
P25@graphene@Fe_3O_4	Solvothermal	5.26	RhB, MB, MO	100	[59]
TiO_2/$CuFe_2O_4$	Sol–gel		MB	57	[60]

manner, other reports also showed the use of silica or carbon as inert layer material between TiO_2 and magnetic core to form composite which was completely magnetically separable with high photocatalytic efficiencies [40–42]. Other material that has been extensively used as photocatalyst is zinc oxide (ZnO), which has a bandgap energy that is similar to that of TiO_2 (3.37 eV). Other benefits that have prompted researchers to extensively study its photoactivity include its electron mobility and inexpensive production costs. Researchers reported the synthesis of Fe_3O_4-embedded ZnO magnetic materials as semiconductor photocatalysts for wastewater treatment. Some other examples of important magnetic metal oxide-based photocatalysts with synthesis method, pollutant, and efficiency of degradation are given in Table 1.

Successful immobilization or covalent bonding of organic moieties and nonmetals, such as S, N, Cl, and P, onto magnetic photocatalysts has also been used to aid in the photodegradation of organic contaminants. It has been demonstrated that adding a well-selected organic modifier can produce a material with a greater

photoactivity than its pure inorganic counterpart. When a material is doped with a suitable dopant, such as N doping in TiO_2 photocatalyst leads to increased photoactivity. The substitution of N-atoms for oxygen in the lattice sites has been connected to an increase in photoactivity, and this will result to an occupied N_{2p} level above valence band of catalyst (O_{2p}). The semiconductor's new N_{2p} level is situated halfway between the valence and conduction bands enabling easier transportation of N_{2p} electrons to conduction band.

The common examples of organic/inorganic/magnetic photocatalysts involve the combination of ferrite with carbon, silica, poly(propylene oxide), polydopamine, poly(N-isopropylacrylamide), multiwalled carbon nanotubes, carbon spheres, graphene, etc., for usage in wastewater treatment via photocatalysis. Along with their appropriate magnetic properties—namely, being ferrimagnetic, ferromagnetic, and super paramagnetic (nanoparticle size < 10 nm)—their synthesis process is easy and inexpensive. According to their intended usage, these magnetic materials' size, shape, and magnetism may be easily changed, making it simple to disperse them in liquid media and maintain their stability for various applications. Additionally, these materials are biocompatible, chemically inert, thermally stable, and non-toxic or less hazardous [2].

In addition, numerous researches have been conducted in which the various magnetic properties, such as electron spin, external magnetic field, or size/morphology of the catalysts, were identified and might potentially have an impact on the photocatalytic efficiency of the magnetic material.

4 Properties of Magnetic Photocatalysts

The saturation magnetization, coercivity, magnetoresistance effect, etc. of magnetic materials' photocatalysts typically affect their effectiveness. These properties directly affect the rate of charge separation and recombination and hence the photocatalytic efficiency of the material. These properties are directly affected by externally applied magnetic field, tuning of electron spin, and size of the photocatalyst sample. In contrast to expectations, the photocatalytic process takes a period of 10^{-5}–10^{-3} s for the charge separation and transportation of excitons, which is significantly higher than the time of recombination (10^{-12}–10^{-3} s) in a typical semiconductor [61]. Here, the preparation of composite materials would solve the splitting and transfer of photoexcited electron–hole pairs-related issues. When a metal and semiconductor are combined, the semiconductor's energy band forms an interfacial electronic antiblocking layer, delaying the recombination of excitons. This results from the disparity between the Fermi level of the semiconductor and the work function of the metal. Another method to improve the separation and transmission of photogenerated electron–hole pairs is to apply an external magnetic field while the photocatalytic process is underway.

External magnetic field and Electron spin orientation

An acceptable, effective, non-contact way for increasing photocatalytic efficiency is to apply an external magnetic field. The magnetic field can alter the electrical configurations of the photocatalyst in its ground state, specifically the direction of the electron spin, in addition to producing the Lorentz force to split the photogenerated electrons and holes. Additionally, the chance that reaction intermediates will come into contact with catalyst-active sites is increased by an external magnetic field.

In case of non-ferromagnetic materials, external magnetic field does not impact electron spin orientation, and both show separate effect on the photocatalytic efficiency of the materials. When an external magnetic field is applied, a moving charged species in a magnetic field encounters a Lorentz force for non-ferromagnetic materials. Lorentz force is determined by the equation $F = q.v.B$, where q is the charge, v is the velocity, and B is the strength of the magnetic field. Light activates the electron–hole pairs during the photocatalytic reaction. They will experience opposing forces and deviate in the opposite direction when traveling in an external magnetic field as a result of their opposite charges. More carriers can interact with the catalyst surface and take part in the catalytic activity as a result of the longer lifetimes of electrons and holes.

Since charge and spin are two characteristics that electrons inherently possess. Spin orientations can be categorized as upward and downward, and inverse spin orientations will produce magnetic fields in the opposite direction. The electron spin states within a catalyst determine the electronic configurations of the catalyst's ground state, which in a notable way influence a catalyst's ability to absorb light, photogenerated carriers' splitting and recombination, and the intermedia species reaction barrier. Enhancing the effectiveness of electron transfer is possible through the dissipation-less spin transporting generated by spin polarization. Spin orientation can be tuned by adjusting the vacancies available in the catalyst via doping. In case of ferromagnetic sample, the spin orientation can be simply tuned by applying external magnetic field [62].

Electron spin states and outside magnetic fields have an impact on photocatalysis performance when ferromagnetic catalysts are exposed to a magnetic field. Electrons with spin preference can be produced by ferromagnetic catalysts, and these electrons will align with the external magnetic field. The interface of composite catalysts could easily permit the passage of electrons with precise spin alignments. A common trait is a negative magnetoresistance (MR) effect. The formula for MR can be given in Eq. (5) below:

$$\mathrm{MR} = [(R_H - R_0)/R_0] \times 100\%, \tag{5}$$

where the symbols R_H and R_0, respectively, stand for the resistances with and without a magnetic field. A substance exhibiting the MR effect can change its resistance when the magnetic field is present. Therefore, the resistance will drop in a magnetic field if a photocatalyst material displays a negative MR effect. A negative MR photocatalytic material will have its spin moments align parallel to one another in the presence

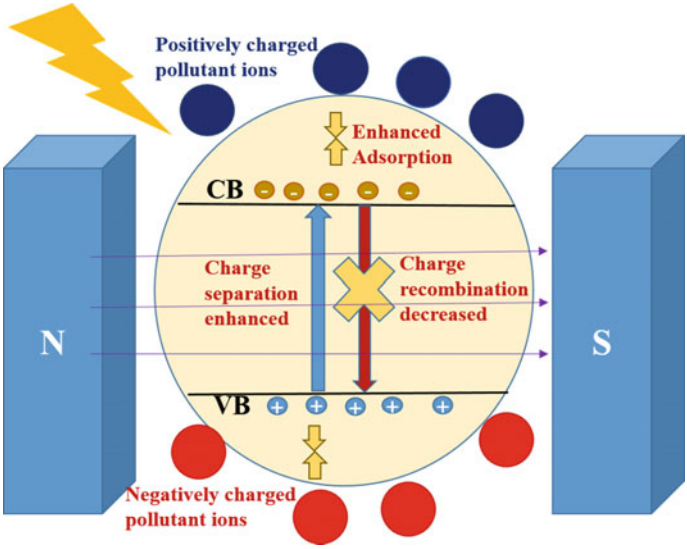

Fig. 5 Schematic of improved charge separation and enhanced photocatalysis via application of external magnetic field

of a magnetic field, which allows for more photogenerated carriers to participate in the surface photocatalytic processes. As a result, photogenerated carriers will be used more frequently, and photocatalytic performance will be improved with high sunlight conversion efficiency. In the meanwhile, a magnet can easily recycle photocatalysts having ferromagnetic properties [61, 63]. The schematic of charge separation with induced Lorentz force by applying external magnetic field and thus leading to enhanced photocatalytic activity is shown in Fig. 5.

Shi et al. [61] reported that hydrothermal and photoreduction methods used to create $ZnFe_2O_4$/Ag were used to deposit it on a 3D-cs substrate (to create 3D-cSZA) for increased surface area. In a 3D-cSZA photodegradation experiment, MO degraded 18% within 90 min and the photodegradation performance is further enhanced by the addition of a magnetic field, and at the same time, 24% of MO was degraded. Due to the photocatalyst's negative magnetic resonance (MR), when a magnetic field is provided, excessive electrons and holes can move to the surface to degrade pollutants, which are advantageous for increasing photocatalytic efficiency. Li et al. [64] reported the photocatalytic removal of Rhodamine B dye at equivalent rates of 59%, 74%, 83%, and 84% (magnetic fields 0, 3, 6, and 8 kOe, respectively) in the presence of α-Fe_2O_3/rGO nanocomposites. The applied magnetic field led to a notable increase in photocatalytic efficiency. In contrast, the photocatalytic efficiency of pure α-Fe_2O_3 was barely observed at zero magnetic field. When the α-Fe_2O_3/rGO nanocomposites were subjected to various magnetic fields, an apparent MR effect can be seen. While α-Fe_2O_3 nanoparticles did not exhibit MR impact due to alignment of magnetic

moment (α-Fe_2O_3 + rGO) and applied magnetic field lines, electronic spin orientation could easily pass through the resulted interface, which resulted in lowered resistance of α-Fe_2O_3/rGO nanocomposites when a magnetic field was applied. In a similar work, Wang et al. [65] used the composite photocatalyst of α-Fe_2O_3 and rGO (mass ratio, 10:1) in 1000 Oe magnetic field. The visible light-induced degradation efficiency of Congo red (CR) was improved from 60 to 87%. In comparison to pure α-Fe_2O_3, the composite photocatalyst had a greater negative MR and more vigorous magnetization intensity, according to magnetic behavior measurement. By applying a magnetic field, it was possible for the electrons with the precise spin alignments to flow over the contact with ease. He et al. [63] prepared $ZnFe_2O_4$/AgBr magnetic photocatalyst. The % degradation of Congo red using the synthesized photocatalyst without the external magnetic field was 40% in 90 min. The photodegradation efficiency of $ZnFe_2O_4$/AgBr was significantly increased by applying 1000 Oe of magnetic field; 53% of condo red was photodegraded in just 90 min. It was observed that only AgBr catalyst showed no changes in their photocatalytic efficiency with variation in magnetic field. Also, pure $ZnFe_2O_4$ showed significant enhancement in the photoactivity with external applied magnetic field. Therefore, it was concluded that due to its greater negative MR, $ZnFe_2O_4$/AgBr has the maximum photocatalytic activity when exposed to a magnetic field.

Hence, adding the magnetic field to photocatalytic processes is a useful and effective way to increase the efficiency of solar energy conversion while also improving adsorption on surfaces and charge separation.

Size and Morphology

The particle size induced magnetic features, e.g., coercivity and saturation magnetization, has already been well-documented. Depending on the material, saturation magnetization and coercivity for small nanoparticles up to a threshold size have been observed to increase as particle size has risen. The following equation gives the separating magnetic force (F_m) operating on the particles from solution with the help of external magnetic field:

$$F_m = \mu_0 . V_p . (M_p . N) H_a, \tag{6}$$

where V_p and M_p are the particle's volume and magnetism, respectively, and H_a is applied magnetic field strength. Therefore, the force needed to separate the magnetic particles from the solution increases with respect to increased particle size. The surface-to-volume ratio is decreased by increasing particle diameter, which lowers the photocatalytic material's effectiveness. So, in order to obtain the desired outcomes in these methods: improved photochemical kinetics and magnetic recovery, these parameters must be regulated [66].

The factors such as size, coercivity, saturation magnetization, which directly affect their performance, are influenced by the morphology of the nanoparticles in addition to the size and nature of the material. Exploring various nanomaterials morphologies is therefore vital to fully comprehend the potential benefits and drawbacks that each

one of them may have in relation to applications. The foundation for the development of advanced multicomponent magnetic systems will be the structure–properties relationship as well as the selection of synthesis techniques in terms of resilience, particle size uniformity, scalability, and chemical characteristics. The saturation magnetization directly affects the magnetic moment which in turns consequences the photocatalytic activity of the magnetic materials. An increase in photocatalytic degradation is related to the maximum net magnetic moment [67]. The cube-shaped particles exhibit the highest saturation magnetization, while rod-like particles exhibit the lowest, notwithstanding the difficulty in accurately controlling the morphology, particle size, and crystallinity of the nanosized particles [68]. Baghshahi et al. [68] reported that after 120 min of exposure to light, the photocatalytic MB removal efficiency of Fe_3O_4-TiO_2 NPs was greater than 90, 73, and 64% (spherical, cube, and rods, respectively). On the contrary, in another report by Baghshahi et al. [69], magnetite nanoparticles of different morphologies were developed by hydrothermal method with magnetic saturation of 60.74, 66.36, and 35.11 emu/g for the sphere, cube, and rod-like morphologies. The results were interpreted in terms of particle size, and the greater critical size of rod-shaped nanoparticles can be used to explain the magnetic drop in saturation. In contrast to spherical nanoparticles, the magnetic saturation of cubic nanoparticles rises with size.

Only a very few reports are available in which the effect of morphology in correlation with particle size of magnetic materials on their photocatalytic activity is explained. The variation in morphology contributes in the saturation magnetization of the magnetic material which in turn affects its photocatalytic activity, but the results are dependent on particle size too. In conclusion, both particle size and morphology play altogether to put an impact on the saturation magnetization and thus photocatalytic activity of the magnetic material.

5 Conclusion

This chapter explains how magnetic materials' structure–property connection affects their photocatalytic efficiency for removing organic contaminants from aqueous solutions. The availability of drinkable water is still a problem for mankind, aquatic vegetation, and animals. In this context, research teams have found a number of techniques for recycling spent water. Among them, the oxidation of organic pollutants (such as dyes, pigments, pesticides) by photocatalysis appears simple and quick, and it produces non-toxic by-products. The role of semiconducting magnetic nanoparticle in the photocatalysis has been explained in detail. Different types of magnetic materials, viz ferrites, their organic, inorganic, metallic composites, and their role in photocatalysis have been discussed thoroughly. However, a very few researchers studied the influence of these catalysts' magnetic properties on photocatalytic activity. In case of non-ferromagnetic materials, external magnetic field does not impact electron spin orientation, and both show separate effect on the photocatalytic efficiency of the materials. Electron spin states and outside magnetic fields have an impact on the

efficiency of photocatalysis when ferromagnetic catalysts are exposed to a magnetic field. Spin-preferential electrons can be produced by ferromagnetic catalysts, and these electrons will align with the surrounding magnetic field. The common trait is negative MRs. More photogenerated carriers can take part in the surface photocatalytic processes because a negative MR photocatalytic material will have its spin moments align parallel to one another in the presence of a magnetic field. As a result, photogenerated carriers will be used more frequently, and high sunlight conversion efficiency will enhance photocatalytic activity. Other than external magnetic field, effect of particle size and morphology on their photocatalytic activity was also discussed. It was concluded that the variation in morphology influences the saturation magnetization of the magnetic material, which in turn impacts its photocatalytic activity, but the outcomes also depend on particle size. To achieve a suitable magnetic performance for such photocatalytic applications, magnetic particles must be of the appropriate sizes and have a morphology that exhibits high saturation magnetization.

References

1. Saharan VK, Pinjari DV, Gogate PR, Pandit AB (2014) Advanced oxidation technologies for wastewater treatment: an overview. Elsevier Ltd
2. Sharma M, Kalita P, Senapati KK, Garg A et al (2016) Emerging pollutants—some strategies for the quality preservation of our environment, vol 11, pp 61–78
3. UNICEF. https://www.unicef.org/wash/water-scarcity
4. WHO. https://www.who.int/news-room/fact-sheets/detail/drinking-water
5. Song X, Wang Y, Wang K, Xu R (2012) Ind Eng Chem Res 51:13438
6. Yin J, Pei M, He Y, Du Y, Guo W, Wang L (2015) RSC Adv 5:89839
7. Konicki W, Cendrowski K, Bazarko G, Mijowska E (2015) Chem Eng Res Des 94:242
8. Bedin KC, Martins AC, Cazetta AL, Pezoti O, Almeida VC (2016) Chem Eng J 286:476
9. Kundu S, Chowdhury IH, Naskar MK (2018) J Chem Eng Data 63:559
10. Lazo-Cannata JC, Nieto-Márquez A, Jacoby A, Paredes-Doig AL, Romero A, Sun-Kou MR, Valverde JL (2011) Sep Purif Technol 80:217
11. Chen A, Li Y, Yu Y, Li Y, Xia K, Wang Y, Li S, Zhang L (2016) Carbon N Y 103:157
12. Song X, Gunawan P, Jiang R, Leong SSJ, Wang K, Xu R (2011) J Hazard Mater 194:162
13. Gong J, Liu T, Wang X, Hu X, Zhang L (2011) Environ Sci Technol 45:6181
14. Quach-Cu J, Herrera-Lynch B, Marciniak C, Adams S, Simmerman A, Reinke RA (2018) Water 10:13
15. Jayalekshmi JS, Minnu Biju SJ, Ajas DS, Muhammad PE (2021) Int J Eng Res Technol 1:3
16. Zhu M, Lee L, Wang H, Wang Z (2007) J Hazard Mater 149:735
17. Abid MF, Zablouk MA, Abid-Alameer AM (2012) J Environ Heal Sci Eng 9:1
18. Teh CY, Budiman PM, Shak KPY, Wu TY (2016) Ind Eng Chem Res 55:4363
19. Banerjee S, Sharma GC, Gautam RK, Chattopadhyaya MC, Upadhyay SN, Sharma YC (2016) J Mol Liq 213:162
20. Atchariyawut S, Phattaranawik J, Leiknes T, Jiraratananon R (2009) Sep Purif Technol 66:153
21. Vlyssides AG, Loizidou M, Karlis PK, Zorpas AA, Papaioannou D (1999) J Hazard Mater B70:41
22. Qu Y, Shi S, Ma F, Yan B (2010) Bioresour Technol 101:8016
23. Nageeb M (2013) Organic pollutants—monitoring, risk and treatment
24. Ren G, Han H, Wang Y, Liu S, Zhao J, Meng X, Li Z (2021) Nanomaterials 11
25. Ambashta RD, Sillanpää M (2010) J Hazard Mater 180:38

26. Zielińska-Jurek A, Bielan Z, Dudziak S, Wolak I, Sobczak Z, Klimczuk T, Nowaczyk G, Hupka J (2017) Catalysts 7
27. Masunga N, Mmelesi OK, Kefeni KK, Mamba BB (2019) J Environ Chem Eng 7:103179
28. Abdel Maksoud MIA, Fahim RA, Bedir AG, Osman AI, Abouelela MM, El-Sayyad GS, Elkodous MA, Mahmoud AS, Rabee MM, Al-Muhtaseb AH, Rooney DW (2022) Engineered magnetic oxides nanoparticles as efficient sorbents for wastewater remediation: a review, vol 20. Springer International Publishing
29. Orge CA, Soares OSGP, Ramalho PSF, Pereira MFR, Faria JL (2019) Catalysts 9
30. Singh P, Sharma K, Hasija V, Sharma V, Sharma S, Raizada P, Singh M, Saini AK, Hosseini-Bandegharaei A, Thakur VK (2019) Mater Today Chem 14:100186
31. Jacinto MJ, Ferreira LF, Silva VC (2020) J Sol-Gel Sci Technol 96:1
32. Wu T, Liu L, Pi M, Zhang D, Chen S (2016) Appl Surf Sci 377:253
33. Díez AG, Rincón-Iglesias M, Lanceros-Méndez S, Reguera J, Lizundia E (2022) Mater Today Chem 26
34. Towata A, Sando M (1997)
35. Beydoun D, Amal R, Low GKC, McEvoy S (2000) J Phys Chem B 104:4387
36. Abbas M, Parvatheeswara Rao B, Reddy V, Kim C (2014) Ceram Int 40:11177
37. Wei JH, Leng CJ, Zhang XZ, Li WH, Liu ZY, Shi J (2009) J Phys Conf Ser 149:012083
38. Zhang L, Wu Z, Chen L, Zhang L, Li X, Xu H, Wang H, Zhu G (2016) Solid State Sci 52:42
39. Gad-Allah TA, Fujimura K, Kato S, Satokawa S, Kojima T (2008) J Hazard Mater 154:572
40. Shi F, Li Y, Zhang Q, Wang H (2012) Int J Photoenergy 2012
41. Fan Y, Ma C, Li W, Yin Y (2012) Mater Sci Semicond Process 15:582
42. Yuan Q, Li N, Geng W, Chi Y, Li X (2012) Mater Res Bull 47:2396
43. Shi L, He Y, Wang X, Hu Y (2018) Energy Convers Manag 171:272
44. Zhao J, Liu J, Li N, Wang W, Nan J, Zhao Z, Cui F (2016) Chem Eng J 304:737
45. Dumitru R, Ianculescu A, Păcurariu C, Lupa L, Pop A, Vasile B, Surdu A, Manea F (2019) Ceram Int 45:2789
46. Surendra BS, Shashi Shekhar TR, Veerabhadraswamy M, Nagaswarupa HP, Prashantha SC, Geethanjali GC, Likitha C (2020) Chem Phys Lett 745:137286
47. Parhizkar J, Habibi MH, Mosavian SY (2019) SILICON 11:1119
48. Bameri I, Saffari J, Baniyaghoob S, Ekrami-Kakhki MS (2022) Colloids interface. Sci Commun 48:100610
49. Li N, Tian Y, Zhao J, Zhan W, Du J, Kong L, Zhang J, Zuo W (2018) Chem Eng J 341:289
50. Karunakaran C, SakthiRaadha S, Gomathisankar P, Vinayagamoorthy P (2013) Powder Technol 246:635
51. Liu X, Zhang T, Xu D, Zhang L (2016) Ind Eng Chem Res 55:11869
52. Jing J, Li J, Feng J, Li W, Yu WW (2013) Chem Eng J 219:355
53. Dong Z, Zhang Q, Chen BY, Hong J (2019) Chem Eng J 357:337
54. Dehghan S, Kakavandi B, Kalantary RR (2018) J Mol Liq 264:98
55. Banerjee S, Benjwal P, Singh M, Kar KK (2018) Appl Surf Sci 439:560
56. Yang Q, Song H, Li Y, Pan Z, Dong M, Chen F, Chen Z (2017) J Mol Liq 234:18
57. Yingzhe Z, Yuxing H, Qingdong Q, Fuchun W, Wankun W, Yongmei L (2018) Superlattices Microstruct 118:123
58. Sun M, Han X, Chen S (2019) Mater Sci Semicond Process 91:367
59. Cheng L, Zhang S, Wang Y, Ding G, Jiao Z (2016) Mater Res Bull 73:77
60. Li H, Zhang Y, Wang S, Wu Q, Liu C (2009) J Hazard Mater 169:1045
61. Shi C, Wang Y, He J, Feng D, Zhang R, Zheng L, Yang Z, Li H, Pan P, Zhao J, Zhang K, Cheng Y, Liu H (2022) Ceram Int 48:32314
62. Peng C, Fan W, Li Q, Han W, Chen X, Zhang G, Yan Y, Gu Q, Wang C, Zhang H, Zhang P (2022) J Mater Sci Technol 115:208
63. He J, Wang Y, Shi C, Wang M, Cao Z, Zhang R, Sun X, Bo J, Li W, Yang Z, Feng D, Zheng L, Pan P, Li H, Bi J, Zhao J, Zhang K, Cheng Y, Liu H (2022) Sep Purif Technol 284:120263
64. Li J, Pei Q, Wang R, Zhou Y, Zhang Z, Cao Q, Wang D, Mi W, Du Y (2018) ACS Nano 12:3351

65. Wang Y, Wang S, Wu Y, Wang Z, Zhang H, Cao Z, He J, Li W, Yang Z, Zheng L, Feng D, Pan P, Bi J, Li H, Zhao J, Zhang K (2021) J Alloys Compd 851:156733
66. Gómez-Pastora J, Dominguez S, Bringas E, Rivero MJ, Ortiz I, Dionysiou DD (2017) Chem Eng J 310:407
67. Cervera-Gabalda L, Zielińska-Jurek A, Gómez-Polo C (2022) J Magn Magn Mater 560:0
68. Baghshahi S, Yousefi F (2022) Trans Indian Ceram Soc
69. Baghshahi S, Yousefi F (2021) J Supercond Nov Magn 34:1949